J Neurophysiol 123: 473–483, 2020.
First published December 11, 2019; doi:10.1152/jn.00589.2019.

RESEARCH ARTICLE | *Sensory Processing*

Luminance potentiates human visuocortical responses

Louis N. Vinke[1,3] and Sam Ling[2,3]

[1]*Graduate Program for Neuroscience, Boston University, Boston, Massachusetts;* [2]*Psychological and Brain Sciences, Boston University, Boston, Massachusetts; and* [3]*Center for Systems Neuroscience, Boston University, Boston, Massachusetts*

Submitted 13 September 2019; accepted in final form 6 December 2019

Vinke LN, Ling S. Luminance potentiates human visuocortical responses. *J Neurophysiol* 123: 473–483, 2020. First published December 11, 2019; doi:10.1152/jn.00589.2019.—Our visual system is tasked with transforming variations in light within our environment into a coherent percept, typically described using properties such as luminance and contrast. Models of vision often downplay the importance of luminance in shaping cortical responses, instead prioritizing representations that do not covary with overall luminance (i.e., contrast), and yet visuocortical response properties that may reflect luminance encoding remain poorly understood. In this study, we examined whether well-established visuocortical response properties may also reflect luminance encoding, challenging the idea that luminance information itself plays no significant role in supporting visual perception. To do so, we measured functional activity in human visual cortex when presenting stimuli varying in contrast and mean luminance, and found that luminance response functions are strongly contrast dependent between 50 and 250 cd/m^2, confirmed with a subsequent experiment. High-contrast stimuli produced linearly increasing responses as luminance increased logarithmically for all early visual areas, whereas low-contrast stimuli produced either flat (V1) or assorted positive linear (V2 and V3) response profiles. These results reveal that the mean luminance information of a visual signal persists within visuocortical representations, potentially reflecting an inherent imbalance of excitatory and inhibitory components that can be either contrast dependent (V1 and V2) or contrast invariant (V3). The role of luminance should be considered when the aim is to drive potent visually evoked responses and when activity is compared across studies. More broadly, overall luminance should be weighed heavily as a core feature of the visual system and should play a significant role in cortical models of vision.

NEW & NOTEWORTHY This neuroimaging study investigates the influence of overall luminance on population activity in human visual cortex. We discovered that the response to a particular stimulus contrast level is reliant, in part, on the mean luminance of a signal, revealing that the mean luminance information of our environment is represented within the visual cortex. The results challenge a long-standing misconception about the role of luminance information in the processing of visual information at the cortical level.

human neuroimaging; luminance; luxotonicity; vision; visual cortex

INTRODUCTION

Standard models of vision propose that certain selective properties are vital for forming coherent percepts, including orientation (Graham et al. 1993; Hubel and Wiesel 1968; Ling et al. 2009), spatial frequency (Watanabe et al. 1968; Wilson et al. 1983), and contrast (Albrecht and Geisler 1991) – all serving as building blocks for neural representations of visual scenes. Contrast, a cornerstone visual feature (Blakeslee and McCourt 2004; Cohen and Grossberg 1984), is derived from the variation in intensity around the mean luminance of a visual signal. Although this relative measure discounts the contribution of overall luminance from the neural code at the cortical level, we regularly encounter visual scenes with components portraying little or no local contrast modulation, such as tabletops or a clear sky. In these cases, the visual system would conceivably need to rely heavily on a more appropriate measure of the visual scene, such as the mean luminance, to generate a well-informed percept. Indeed, statistical regularities found within natural scenes demonstrate that luminance and relative contrast information are largely independent properties (Frazor and Geisler 2006; Mante et al. 2005), indicating analogs for both properties should be encoded to generate an accurate percept of our everyday environment. Moreover, studies of perceived lightness have demonstrated that humans are sensitive to luminance differences, even in the absence of local contrast information (Barlow and Verrillo 1976; Gilchrist et al. 1983).

Despite the functional utility that luminance coding may serve in supporting our visual perception, very few studies have considered the idea that mean luminance information persists within the visual signal, propagating to the visual cortex. This is likely due to the commonly held dogma that mean luminance is discounted at the retinal level (Cornsweet 1970; Kingdom 2011). Standard models of vision largely depend on the center-surround organization of receptive fields, wherein changes in the overall luminance of a stimulus would predict no change in neural response. There is, however, some evidence to suggest this is not the case: a collection of animal electrophysiological studies have identified a minority of individual striate units possessing luxotonic response profiles, where firing rates are found to change monotonically with increases in luminance (Bartlett and Doty 1974; Kayama et al. 1979; Kinoshita and Komatsu 2001; Peng and Van Essen 2005; Rossi and Paradiso 1999). In animals, the mean luminance of a stimulus also appears to influence responses to other core visual features, namely, contrast (Bisti et al. 1977; Geisler et al. 2007; Wang et al. 2015). However, although these animal studies have found evidence in support of luminance-based responses, the prevalence of these responses remains controversial, often varying from species to species (DeYoe and

Address for reprint requests and other correspondence: L. Vinke, 677 Beacon St., Boston, MA 02215 (e-mail: vinke@bu.edu).

Bartlett 1980; Kahrilas et al. 1980; Squatrito et al. 1990). More recently, a minority of functional neuroimaging studies have begun to investigate the effect of overall luminance on visuocortical responses in humans, providing mixed evidence for luxotonic responses within early visual cortex (Boyaci et al. 2007; Cornelissen et al. 2006; Goodyear and Menon 1998; Haynes et al. 2004).

In this study, we used functional magnetic resonance imaging (fMRI) to examine the existence of luminance-driven population responses within human visual cortex and determine whether there exists any systematic organization of luminance response, both within and across early visual areas. Moreover, we assessed the degree to which luminance interacts with contrast. Our findings revealed that luminance-based responses are quite robust throughout early human visual cortex and are expressed by an active interaction with cortical contrast responses, predominantly at higher contrast levels within a particular luminance regime well within the photopic range. These results suggest that by acting on cortical processes and representations in the human visual cortex, overall luminance may indeed influence human behavior and perception and should be considered a core feature in cortical models of vision.

MATERIALS AND METHODS

Participants. All eight participants (5 women) in this study were between the ages 18 and 35 yr, reported normal or corrected-to-normal visual acuity, and were recruited from Boston University and the surrounding community. All participants provided written informed consent before study enrollment and were required to complete a metal screening form indicating they had no MRI-related contraindications. Participants were reimbursed for volunteering their time. All aspects of the study were approved by the Boston University Institutional Review Board. *Experiment 1* had a total of seven participants, whereas *experiment 2* had a total of six participants. Of the seven participants recruited for *experiment 1*, five of them also participated in *experiment 2*.

Visual stimuli. Stimuli were generated using MATLAB (version 2015b), in conjunction with the Psychophysics toolbox (Brainard 1997). Participants viewed stimuli that were back-projected onto a screen set within the MRI scanner bore, using an InFocus IN5542 projector (minimum luminance: 1.2 cd/m^2 or 3.8 Td; maximum luminance: 2507.9 cd/m^2 or 7,878.8 Td), which permitted the investigation of a much larger dynamic range of luminance levels than in previous studies, a range that better approximated the natural luminance levels our visual system is exposed to in natural environments (Xiao et al. 2002). Photometer measurements (model LS-100; Konica Minolta) carried out before the study were used to linearize luminance display values [1 digital-to-analog conversion (DAC) step = 9.835 cd/m^2 or 30.9 Td]. These measurements, which were also used to calculate stimulus luminance and contrast levels, were acquired from the inner-facing side of a back-projection screen while positioned within the MRI scanner bore, replicating the viewing conditions during functional data collection. This was done so that any attenuation in luminance due to back-projection screen characteristics, or light scatter within the projector optics, was accounted for as best as possible. To control for changes in spherical aberrations, brought about by pupillary light reflexes (Schweitzer 1956), participants viewed the stimuli monocularly (right eye only) through an in-house fabricated artificial pupil aperture (Fig. 1*A*). The diameter of the

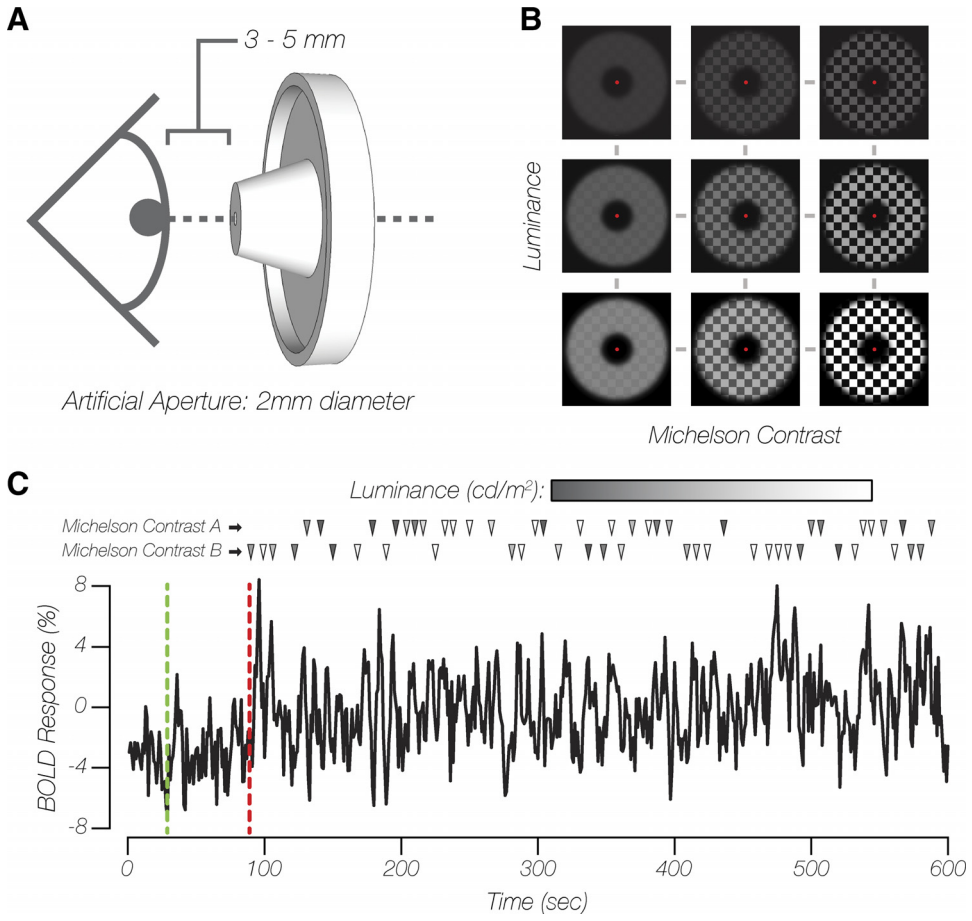

Fig. 1. Experimental stimulus presentation. *A*: schematic of artificial pupil aperture positioning. *B*: examples of checkerboard pattern stimuli, varying in overall luminance and contrast (actual stimulus spatial frequency not depicted). *C*: exemplar single-voxel blood oxygen level-dependent (BOLD) signal time series of a single functional magnetic resonance imaging (fMRI) run from *experiment 1*. Green and red dashed lines indicate the end of the baseline and adaptation periods, respectively. The remainder of each fMRI run consisted of jittered stimulus presentations for a pair of contrast conditions at all luminance levels. Each row of triangles denotes the onsets of each stimulus contrast type, with shading of each triangle corresponding to the luminance of that particular stimulus.

aperture within the artificial pupil was fixed at 2 mm, which was assessed as smaller than the smallest pupillary constriction, given the luminance of the visual input and mean age of participants (Watson and Yellott 2012). Modified goggles and orthopedic putty were used to cradle the artificial pupil, positioning the aperture 3–5 mm from the participants' pupils. Care was taken to eliminate any stray sources of light, including turning off the MRI scanner bore lights. All participants reported that they were able to clearly see the majority of the projected image on the screen within the scanner bore.

Throughout the experiment, participants fixated on a 0.175° dot at central fixation while viewing a checkerboard pattern (fundamental spatial frequency of 0.75 cycles/deg, 10-Hz counter-phase flicker frequency). The checkerboard stimuli were presented with parametric combinations of mean luminance and Michelson contrast [$(Max_L - Min_L)/(Max_L + Min_L)$, where Max_L is maximum luminance and Min_L is minimum luminance]. In *experiment 1*, stimulus mean luminance was linearly spaced above and below 757.3 cd/m^2 (within session: 49.2, 226.2, 403.2, 580.3, 757.3, 885.2, 1,022.8, 1,150.7, and 1,278.6 cd/m^2 or 154.5, 710.6, 1,266.8, 1,823.0, 2,379.1, 2,780.8, 3,213.3, 3,615.0, and 4,016.7 Td) and presented at several Michelson contrast levels (across session: 4, 14, 25, 35, 65, and 96%; Fig. 1*B*). The stimulus was bounded by two circular apertures (inner diameter = 5°, outer diameter = 18°), creating an annulus-shaped stimulus with a 6.5° width. In *experiment 2*, stimulus mean luminance was logarithmically spaced between 50 and 250 cd/m^2 (within session: 49.2, 68.9, 98.4, 137.7, 186.9, and 245.9 cd/m^2 or 154.5, 216.3, 309.0, 432.6, 587.1, and 772.4 Td) and presented at the two extreme Michelson contrast levels (within session: 4 and 96%) from *experiment 1*. The stimulus was bounded by two circular apertures (inner diameter = 1.5°, outer diameter = 18°), creating an annulus-shaped stimulus with an 8.25° width. The stimulus inner diameter was decreased so as to increase the number of visuocortical voxel responses selected for the functional data analysis in *experiment 2* relative to *experiment 1*. For both experiments, a Gaussian roll-off was imposed at the borders with the black background, which smoothed the boundaries between the stimulus and the background.

Experimental design. All data for both experiments were acquired over five 2-h scan sessions. Four sessions were dedicated to collecting fMRI blood oxygen level-dependent (BOLD) data across various experimental conditions (for *experiments 1* and *2*). The fifth session was dedicated to collecting anatomical images and data for population receptive field (pRF) mapping using standard techniques and stimuli (Dumoulin and Wandell 2008; Kay et al. 2013; Kriegeskorte et al. 2008).

For each of the four fMRI experimental condition sessions, participants completed 5–7 runs of a 10-min event-related fMRI experiment, resulting in a minimum of 15 observations per parametric stimulus combination in both *experiments 1* and *2*. For both experiments, each run consisted of three stages presented in the following order (Fig. 1*C*): *1*) a 30-s baseline period, during which participants viewed a uniform gray background (757.3 cd/m^2); *2*) a 60-s period, during which participants were adapted to a low-contrast (4%) checkerboard stimulus; and *3*) an 8.5-min rapid event-related presentation of experimental stimuli (2 s in duration), with each presentation intermixed with an adaptation top-up stimulus (4–20 s in duration; visual properties identical to the initial adaptation period stimulus). The experimental stimulus presentation timing was generated using the Optseq2 schedule optimization tool (Dale 1999). A 60-s initial adaptation period was previously shown to induce a stable adapted state of the human visual system (Blakemore and Campbell 1969). Because data collection took place over multiple sessions and there were small differences in average image statistics (i.e., contrast) across sessions, we selected a low-contrast adapter stimulus and a relatively short duration of experimental stimuli compared with the average top-up adapter duration across each experimental run. These design choices were expected to overcompensate for any recovery from adaptation, serving to maintain the initial contrast adaptation state of the visual system throughout each experimental run and scan session (Foley and Boynton 1993; Gardner et al. 2005). Within each functional session, experimental stimuli were presented at all mean luminance levels of interest and at two fixed Michelson contrast levels for *experiment 1* (*session 1*: 4% and 96%; *session 2*: 35% and 65%; *session 3*: 14% and 25%) and *experiment 2* (*session 4*: 4% and 96%). During *sessions 2–4*, the BOLD response to a 0% contrast stimulus at 1.2 cd/m^2 (DAC = 0; 3.8 Td) was also collected to serve as a reference point and was not included in any subsequent model fitting. Throughout each run, participants were engaged in a change-detection task at fixation, where the fixation dot switched between red or white with a 30% probability every 250 ms, after a 1-s delay following the most recent fixation change. Participants used a MR-compatible response box to provide behavioral responses to the change detection fixation task.

MRI data acquisition. All neuroimaging data was acquired using a 64-channel head coil on a research-dedicated Siemens Prisma 3T scanner. A whole brain anatomical scan was acquired using a T1-weighted multiecho MPRAGE three-dimensional sequence [1 mm^3; field of view (FOV) = 256 × 256 × 176 mm, flip angle (FA) = 7°, repetition time (TR) = 2,530 ms, echo time (TE) = 1.69 ms]. All functional MRI scans (pRF mapping, *experiment 1* and *experiment 2*) were acquired using T2*-weighted in-plane simultaneous multislice imaging (multiband factor: 3) (Moeller et al. 2010; Xu et al. 2013), with the field of view oriented perpendicularly to the calcarine sulcus (2 mm^3; FOV = 60 × 112 × 172 mm, FA = 80°, TR = 1,000 ms, TE = 35 ms).

Anatomical data analysis. T1-weighted anatomical data were analyzed using the standard "recon-all" pipeline provided by the FreeSurfer (Fischl 2012) neuroimaging analysis package, generating cortical surface models, whole brain segmentations, and cortical parcellations. Cortical surface models facilitated surface-based registration between structural and functional MRI volumes, allowing pRF analyses to be ported over to native functional volume space.

Functional data analysis. Functional BOLD time-series data were first corrected for echo-planar imaging (EPI) distortions using a reverse phase-encode method (Andersson et al. 2003) implemented in FSL (Smith et al. 2004) and were then preprocessed with FS-FAST (Fischl 2012) using standard motion-correction procedures, Siemens slice timing correction, and boundary-based registration (Greve and Fischl 2009) between functional and anatomical spaces. To optimize voxelwise analyses of experimental data, no volumetric spatial smoothing was performed (full-width half-maximum = 0 mm). To achieve precise alignment of experimental data across and within all three experimental sessions in *experiment 1* and within the one experimental session in *experiment 2*, cross-run within-modality robust rigid registration (Reuter et al. 2010) was performed, using the middle time point of each run. Before BOLD time-series data were converted to units of percent signal change, time points corresponding to the initial adaptation period (60 frames) were excluded. Data collected during the separate pRF mapping scans were analyzed using the analyzePRF toolbox (Kay et al. 2013). Only voxels located within the cortical ribbon were selected for pRF modeling and were identified using an occipital lobe surface label generated using an intrinsic functional connectivity atlas (Yeo et al. 2011).

The results from the pRF modeling were used to identify different region-of-interest (ROI) labels for each experiment before analysis. ROI labels included voxels located inside the cortical ribbon for V1/V2/V3 with eccentricity values falling within experimental stimulus dimensions, compressed by 20% (*experiment 1*: inner diameter = 6°, outer diameter = 14.4°; *experiment 2*: inner diameter = 1.8°, outer diameter = 14.4°). This compression allowed us to avoid inclusion of any voxels that may have been responding to either the inner or outer contours of the experimental stimulus (regions that would contain local contrast differences with changing luminance). ROI labels were further constrained by excluding voxels with poor pRF modeling goodness of fit ($r^2 < 20\%$), unreasonably small population

receptive field sizes (RF $< 0.1°$), and population receptive field sizes larger than the eccentricity range of the compressed ROI bounds (*experiment 1*: RF $> 4.2°$; *experiment 2*: RF $> 6.3°$). The total number of voxels (mean ± SE across participants), after being combined across left and right hemispheres, that survived these criteria were as follows for *experiment 1* (V1: 270 ± 87.9, V2: 253.3 ± 44.5, V3: 181.4 ± 36.9) and *experiment 2* (V1: 524 ± 221.7, V2: 486.2 ± 123.2, V3: 344.7 ± 65.1). The labels and pRF results for these particular voxels were then transformed into each respective native experimental functional volume space for further analysis.

For both experiments, a univariate analysis was performed using a finite-impulse response (FIR) modeling approach (window size = 24 s, prestimulus delay = 4 s), which was agnostic to the shape of the local hemodynamic response function (HRF). This provided a set of 24 beta weight parameters, creating a FIR function describing the HRF response to the presentation of each parametric combination of mean luminance and contrast level under investigation. For each subject, the beta weights were averaged across luminance levels, and the peak was identified as the maximal beta weight poststimulus onset for each contrast level. The average of the five beta weights centered around this peak was used to plot luminance responses and perform further analyses. For the 4% contrast condition, no discernible peak could be identified; therefore, the mean peak across all other contrast levels was used instead.

To easily quantify the degree to which increasing luminance affected the BOLD response in *experiment 2*, linear regression was applied to each set of luminance responses, within each contrast level. The luminance levels were log-transformed first, before the fitting procedure, resulting in $\log_{10}$ luminance as the input variable and BOLD percent signal change as the output variable. This resulted in a set of offset and slope parameters describing the luminance responses for each particular contrast level. This fitting procedure was performed using ROI-based BOLD responses averaged within and across participants (see Fig. 3) and at the voxelwise level for each subject (see Fig. 4).

Statistical analysis. Two-way between-subjects ANOVAs were performed to test for any main effects and interactions of luminance and contrast on BOLD response (*experiments 1* and *2*), as well as contrast-condition slope measurements and voxelwise median slope measurements (*experiment 2* only). The median slope measurement was calculated for each distribution of voxelwise contrast-condition slope estimates across luminance and contrast conditions in *experiment 2*. Circular statistics (angular mean and Rayleigh z test) were performed using the CircStat MATLAB toolbox (Berens 2009) to investigate any topographic organization of luminance-based responses. A one-way ANOVA was performed to test for any systematic differences in functional signal-to-noise (SNR) measurements across visual area ROIs for both *experiments 1* and *2*.

Data and code availability. MATLAB code used for stimulus presentation and data analysis and fMRI data sets used to generate the results reported in this study are available at https://osf.io/t49mr/.

RESULTS

To evaluate whether changes in luminance alter the neural response to a particular Michelson contrast stimulus, we measured the BOLD response to different contrast levels, under several different luminance conditions (Fig. 1*B*), across two fMRI experiments. Visual presentation to participants was constrained using an artificial pupil device (Fig. 1*A*) to control for pupillary reflex confounds. Adaptation was employed across functional sessions to provide a fair comparison of BOLD responses across multiple sessions (Fig. 1*C*).

Human visuocortical contrast responses across extensive luminance range. In *experiment 1*, we measured the BOLD response to six different linearly spaced contrast levels, across nine different luminance conditions (with the exception of the adapter stimulus: 4% contrast response at 757.3 cd/m^2) (Fig. 2). The group-averaged BOLD responses across V1–V3 demonstrated significant main effects of luminance [V1: $F(7, 318) = 11.11$, $P < 0.001$; V2: $F(7, 318) = 17.64$, $P < 0.001$; V3: $F(7, 318) = 12.17$, $P < 0.001$] and contrast [V1: $F(4, 318) = 68.51$, $P < 0.001$; V2: $F(4, 318) = 38.25$, $P < 0.001$; V3: $F(4, 318) = 24.63$, $P < 0.001$]. The interaction between

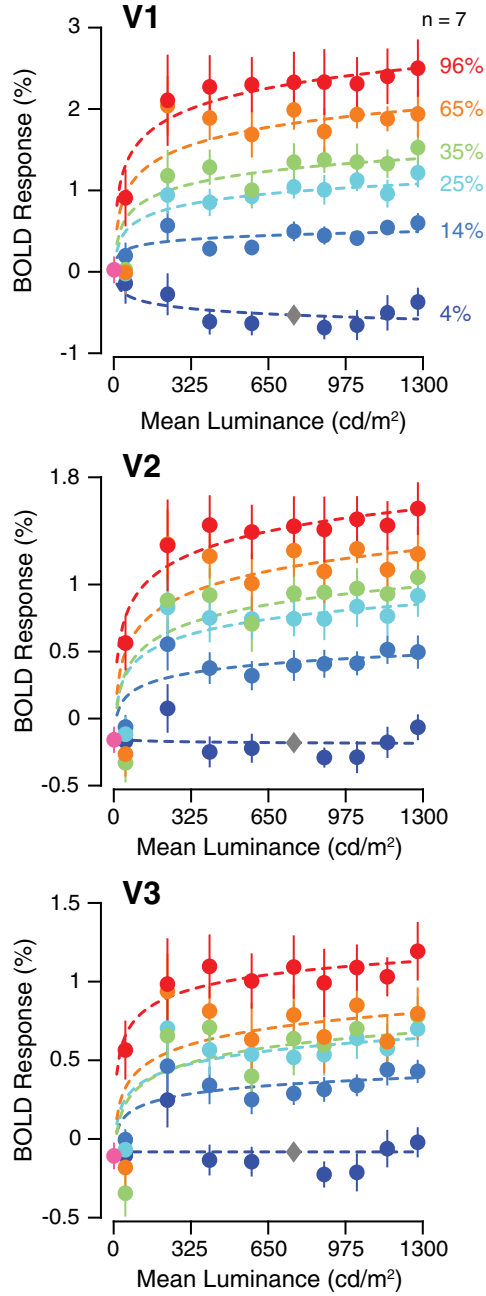

Fig. 2. Visuocortical contrast responses across extensive luminance range (49.2–1278.6 cd/m^2). Data are group-averaged ($n = 7$) blood oxygen level-dependent (BOLD) responses (mean %signal change) for 9 luminance levels and 6 contrast conditions, across early visual cortical regions (V1–V3), displayed with power function fits. The visuocortical response to a full-field "black" screen (1.2 cd/m^2) is represented by a magenta circle. The adapter stimulus response, denoted by a gray diamond, is a predicted response using results of the group-level nonlinear fit estimate for the 4% contrast condition. Data are means ± SE across participants.

luminance and contrast on BOLD response was significant for V1 [$F(39, 318) = 1.46$, $P = 0.043$], but not for V2 [$F(39, 318) = 1.18$, $P = 0.222$] or V3 [$F(39, 318) = 0.88$, $P = 0.684$)]. These results demonstrate that neural population activity in the human visual cortex changes as a function of luminance, an effect that appears to interact with the Michelson contrast of a stimulus only in area V1. It is unclear why contrast responses appear to reach a plateau at higher luminance levels. This plateau could be partially explained by intraocular light scatter producing a disability glare, or a "veil of luminance," effectively increasing the general illumination of the retinal image (Patterson et al. 2015; Vos 2003; Westheimer 2006), in which case the relative contrast of the retinal image would be slightly decreased relative to the displayed stimulus contrast. However, the largest changes in contrast responsivity were observed primarily between 49.2 and 226.2 cd/m^2, for all contrast levels. A second experiment was performed to confirm that the 50-to-250 cd/m^2 luminance range especially promotes strong modulation of contrast responses.

Potentiation of visuocortical contrast responses within focused luminance range. In *experiment 2*, we measured the BOLD response to two different contrast levels, across six different log-spaced luminance conditions, all within the 50-to-250 cd/m^2 luminance range (Fig. 3*A*–*C*). The group-averaged BOLD responses demonstrated a marginally significant main effect of luminance for V1 [$F(5, 60) = 2.16$, $P = 0.071$] and a significant main effect of luminance for V2 [$F(5, 60) = 4.91$, $P < 0.001$] and V3 [$F(5, 60) = 3.12$, $P = 0.014$]. Main effects of contrast on group-averaged BOLD responses were found across V1–V3 [V1: $F(1, 60) = 161.99$, $P < 0.001$; V2: $F(1, 60) = 129.97$, $P < 0.001$; V3: $F(1, 60) = 54.30$, $P < 0.001$]. The interaction between luminance and contrast on BOLD response was significant for V1 [$F(5, 60) = 2.65$, $P = 0.031$], but not for V2 [$F(5, 60) = 1.07$, $P = 0.386$] or V3 [$F(5, 60) = 0.39$, $P = 0.856$]. These results confirm that neural population activity in the human visual cortex is especially susceptible to luminance modulation within the 50-to-250 cd/m^2 luminance range. The ability for luminance to interact with contrast responsivity was only prevalent in striate cortex (V1), despite a signature of luminance modulation persisting across early visual areas. The combination of a (nonsignificant) negative trend of BOLD responses across luminance levels for the 4% contrast condition and the reduced number of contrast conditions in *experiment 2* relative to *experiment 1* most likely accounts for the lack of replication of a significant main effect of luminance on V1 BOLD responses in *experiment 2*.

To better characterize the dynamics between luminance and contrast, linear regression was applied to the luminance response profiles for each of the two contrast conditions in *experiment 2*, producing two slope estimates per ROI and participant. These slope estimates were treated as our measure for the magnitude of luxotonic responses, which we refer to as luxotonicity, where a steep slope is analogous to strong luxotonicity. All luxotonic responses were significantly different from zero, with the exception of the 4% contrast condition in V1 [4% contrast at V1: $t(5) = -1.827$, $P = 0.127$; V2:

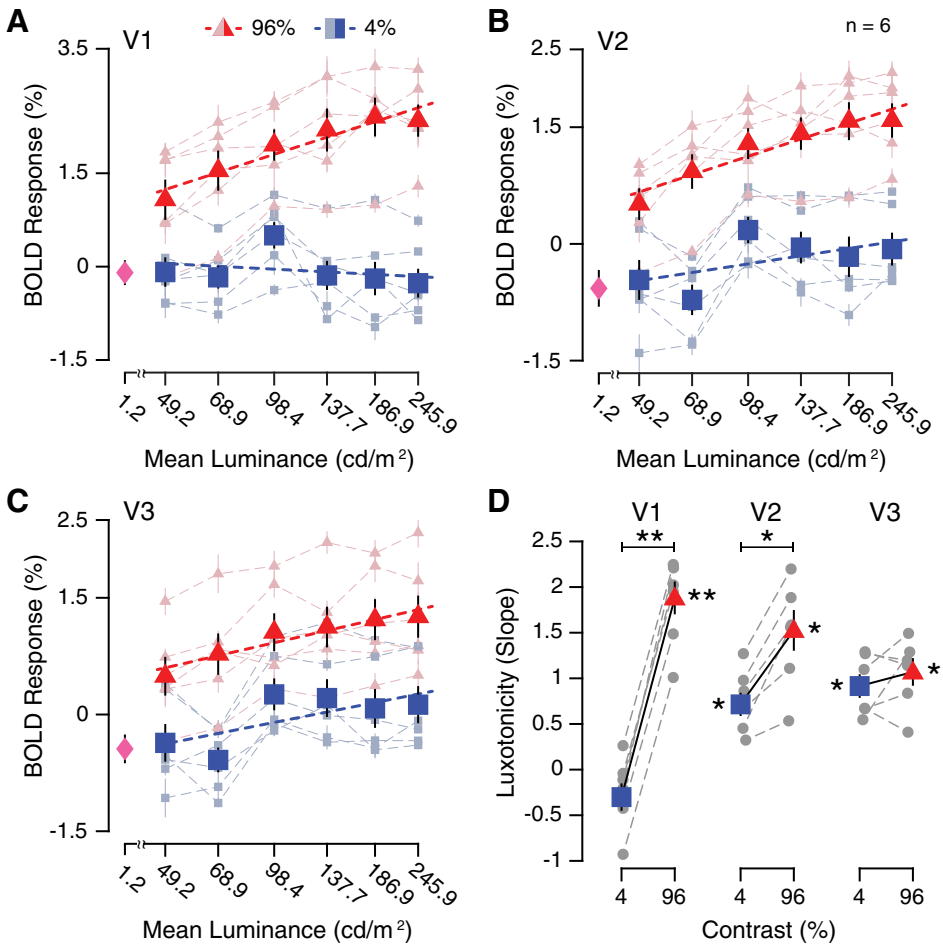

Fig. 3. Potentiation of visuocortical contrast responses within focused luminance range (49.2–245.9 cd/m^2). *A*–*C*: group-averaged ($n = 6$) blood oxygen level-dependent (BOLD) responses (mean %signal change) for 6 luminance levels and 2 contrast conditions, across early visual cortical regions (V1–V3), displayed with linear function fits. The visuocortical response to a full-field "black" screen (1.2 cd/m^2) is represented by a magenta diamond. Shaded symbols and dashed lines represent individual subject luminance response functions. *D*: group-averaged linear regression slope parameters for each contrast condition, across early visual cortical areas (V1–V3). *$P < 0.01$; **$P < 0.001$, significant t test results. Gray symbols and dashed lines represent individual subject slope parameters. Data are means ± SE across participants.

$t(5) = 5.118$, $P = 0.004$; V3: $t(5) = 6.455$, $P = 0.001$; 96% contrast at V1: $t(5) = 9.555$, $P < 0.001$; V2: $t(5) = 6.241$, $P = 0.002$; V3: $t(5) = 6.461$, $P = 0.001$; Fig. 3*D*]. A significant difference in luxotonicity between contrast conditions (4% vs. 96%) was found in V1 [$t(5) = -27.919$, $P < 0.001$] and V2 [$t(5) = -5.416$, $P = 0.002$], but not in V3 [$t(5) = -0.853$, $P = 0.216$]. When these results are considered altogether, they indicate that visuocortical contrast responses change as a function of luminance level. Whereas the impact of luminance on the high-contrast condition is evident throughout early visual cortex, low-contrast stimuli only demonstrate significant changes across luminance levels for V2 and V3.

Luxotonic variability within and across early visual cortex. Within-region effects of luxotonicity were evaluated by utilizing the same linear regression procedure at the voxelwise level for each participant. The median estimates from normalized frequency plots of the voxelwise luxotonicity (slope estimate), for all participants, were used to quantify the prevalence of luxotonicity across contrast levels within each early visuocortical area (Fig. 4). A main effect of contrast on median estimates was found [$F(1, 30) = 47.61$, $P < 0.001$], but no significant difference was found across visual areas [$F(2, 30) = 1.32$, $P = 0.283$]. The interaction between contrast and visual area was significant [$F(2, 30) = 18.45$, $P < 0.001$]. Whereas a large difference in median voxelwise luxotonicity between 4% and 96% contrast conditions was found overall across early visual areas (V1–V3), the median estimates for both contrast conditions converged as the visuocortical hierarchy was ascended. As a whole, the luxotonicity measures found between (Fig. 3*D*) and within (Fig. 4) visual areas indicate that luminance modulation of contrast responses is multiplicative in nature within V1, and to a lesser extent in V2 as well. However, the luminance modulation of contrast responses within V3 is best described as being additive in nature, effectively "discounting the illuminant" by preserving the relative differences in BOLD responsivity between contrast levels.

Retinotopic organization of luxotonicity. To evaluate whether any topographic organization of luxotonicity exists within early visuocortical areas, the slope estimates for the 96% contrast condition from *experiment 2* were examined across retinotopic eccentricity and polar angle dimensions, provided by a population receptive field (pRF) mapping procedure and analysis. No main effect of eccentricity on binned voxelwise luxotonicity was found [$F(5, 90) = 0.358$, $P = 0.876$; Fig. 5*A*]. The lack of any effect of eccentricity on luxotonicity indicates that luxotonic population responses are uniformly distributed within each early visual area (V1–V3). To test whether luxotonicity is anisotropically or uniformly distributed across polar angle, a Rayleigh statistic was computed for all three visual areas using binned voxelwise luxotonicity measurements. Results revealed that no significant unimodal angular peak exists across all visual areas (V1: $\text{Rayleigh}_z = 0.654$, $P = 0.521$; V2: $\text{Rayleigh}_z = 0.007$, $P = 0.993$; V3: $\text{Rayleigh}_z = 0.708$, $P = 0.494$), indicating that luxotonicity is evenly distributed across the visual field in terms of visual angle (Fig. 5*B*). However, it is worth noting that the mean angular biases for luxotonicity across all visual areas were located within the lower visual quadrants (V1: 229.31°; V2: 299.99°; V3: 191.62°).

If luminance-sensitive neural populations are predominantly responsive to components of a visual scene that are uniform in nature (no local contrast) or contain very low spatial frequency characteristics, then these same neural populations may also rely on larger receptive fields over which to integrate to support luminance sensitivity. A main effect of population receptive field (pRF) size on luxotonicity was found [$F(7, 120) = 3.039$, $P = 0.006$], but the interaction with visual area was not significant [$F(14, 120) = 0.722$, $P = 0.749$; Fig. 5*C*]. In general, population receptive field size does predict luxotonicity within each early visual area (V1–V3), but with smaller (<1.3°) pRFs exhibiting the largest luxotonicity, which runs counter to our initial prediction. However, it is interesting to note that the RF cutoff we observed roughly corresponds to the

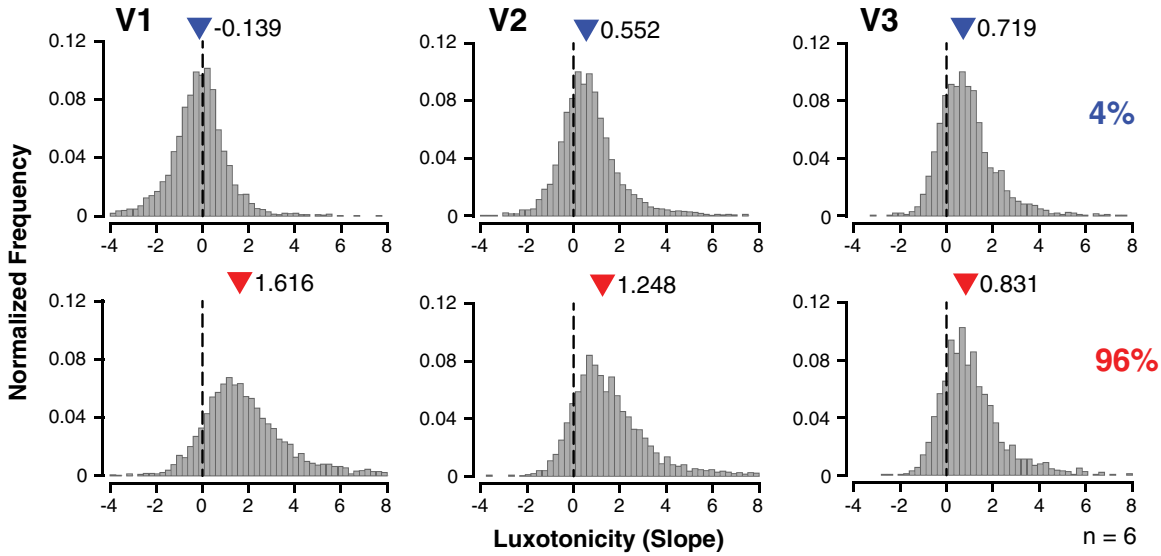

Fig. 4. Variability of voxelwise luxotonic activity within and across early visual cortex. Data are normalized frequency distributions of best-fitting linear regression slope estimates (binwidth = 0.24) demonstrating the variety of luxotonicity at the voxelwise level for all participants ($n = 6$) within early visual cortex (V1–V3). Steeper (more positive) slope estimates indicate a stronger luminance-based response. The median measurement for each distribution is denoted by a colored triangle, along with the specific median measurement. Each row corresponds to a particular contrast condition in *experiment 2*.

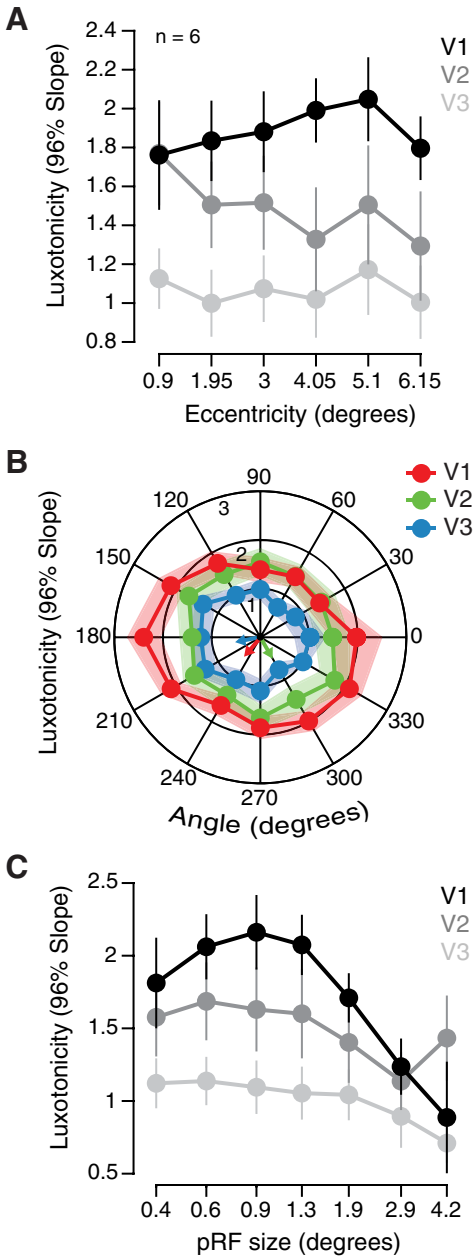

Fig. 5. Retinotopic organization of luxotonicity. *A*: group-averaged (n = 6) luxotonicity plotted as a function of retinotopic eccentricity within early visual cortex. Abscissa represents the minimum value of each bin, with data binned on a linear scale. *B*: group-averaged luxotonicity plotted as a function of retinotopic angle within early visual cortex. Right visual field: 90–270°, clockwise; left visual field: 90–270°, counterclockwise. *C*: group-averaged luxotonicity plotted as a function of population receptive field size (pRF). Abscissa represents the minimum value of each bin, with data binned on a logarithmic scale. Data are means ± SE across participants.

minimum receptive field size necessary to capture one full cycle of the stimulus spatial frequency (0.75 cycle/deg).

Luxotonic effects not explained by SNR differences or ROI selection. The pattern of luxotonicity results seen across ROIs (V1–V3) may have resulted from differences in the SNR of the average BOLD response across areas. When the functional SNR is examined across visual areas in *experiment 1*, no significant differences exist [$F(2, 18) = 1.49$, $P = 0.251$], and the same is found in *experiment 2* [$F(2, 15) = 0.96$, $P = 0.404$]. This indicates that the differences in main effects across visual area reported above are not simply due to monotonic changes in SNR across the visuocortical hierarchy.

To verify that the compressed eccentricity bounds used for defining the subjectwise ROI masks were sufficient to avoid the inclusion of any voxel activity driven by the local contrast differences at the edge of the experimental stimulus, an extremely compressed set of ROI bounds was evaluated. The ROI bounds were compressed by an additional 30%, resulting in a total compression of 50% from the actual stimulus border (*experiment 1*: inner diameter = 7.5°, outer diameter = 9°; *experiment 2*: inner diameter = 2.25°, outer diameter = 9°). The same pattern of significant results was found for the interaction between luminance and contrast on BOLD response as reported above for *experiment 1* [V1: $F(39, 318) = 1.47$, $P = 0.041$; V2: $F(39, 318) = 1.02$, $P = 0.447$; V3: $F(39, 318) = 0.72$, $P = 0.892$] and for *experiment 2* [V1: $F(5, 60) = 2.94$, $P = 0.019$; V2: $F(5, 60) = 1.26$, $P = 0.294$; V3: $F(5, 60) = 0.53$, $P = 0.755$]. The replication of these results obtained when these further constrained eccentricity bounds were used suggests that the original 20% compressed eccentricity bounds were sufficient to avoid any confounds introduced by contrast responses stemming from the local contrast of the inner and outer contours of the experimental stimulus against the black background.

Uniformity of BOLD activity and luxotonicity throughout the stimulus representation. Relatively recent human neuroimaging work has reported an eccentricity bias of the BOLD response when participants viewed center-surround stimuli whose components were uniform in nature (no local contrast) (Cornelissen et al. 2006). In that study, the eccentricity bias was found to exist only at the border between the center and surround components, when each component only contained uniform luminance information. Similarly, the BOLD response within early visual areas has been shown to be strongest at the edge of uniform disk stimuli (Press et al. 2001). However, under certain conditions, larger V1 population responses mapped to the center of uniform stimuli compared against edge responses have been observed in nonhuman primates (Zurawel et al. 2014). A closer inspection of our average BOLD response data and linear regression slope estimates across the entire range of eccentricity from *experiment 2* clearly demonstrates that no peaks exist at the borders of the experimental stimulus or ROI label boundaries (Fig. 6). Therefore, luminance modulation of neural activity in early visual areas is indeed observable across the entirety of a stimulus when stimuli are employed that have adequate local feature properties (i.e., Michelson contrast) which can drive the visual system under static luminance conditions.

DISCUSSION

The results reported in this study provide strong evidence for the existence of luxotonic neural populations in the human visual cortex. By stimulating the human visual system with parametric combinations of luminance and contrast, we discovered that general increases in luminance produce increased BOLD visuocortical responses and that the cortical contrast response interacts with this luminance response, especially within the 50-to-250 cd/m^2 luminance range. The strongest evidence was found in area V1, as a multiplicative interaction,

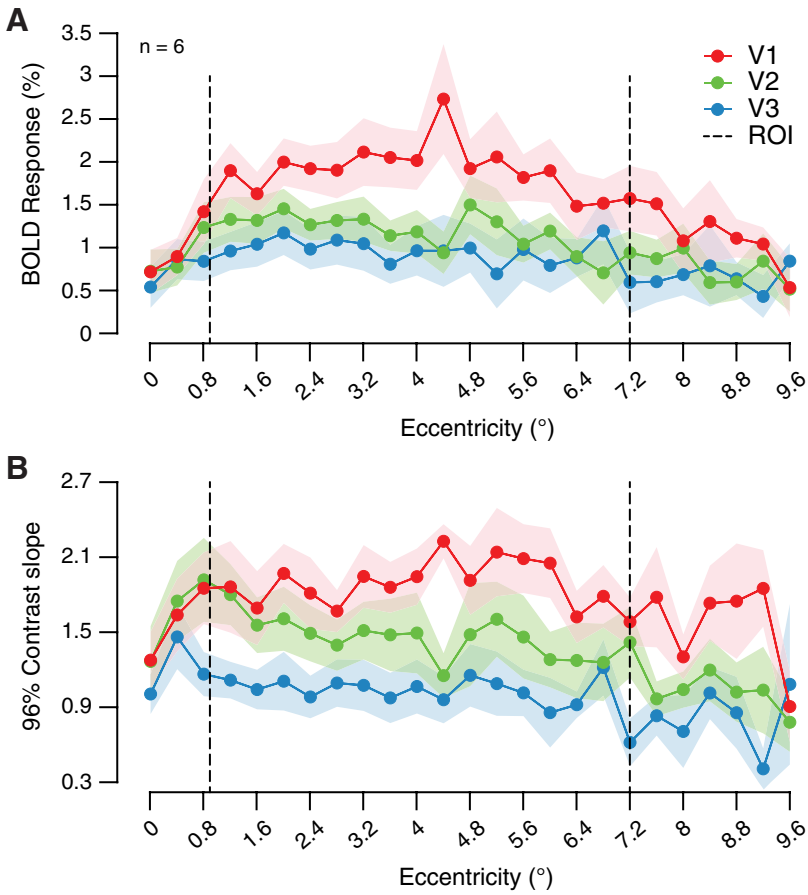

Fig. 6. Uniformity of blood oxygen level-dependent (BOLD) activity and luxotonicity throughout stimulus representation. *A*: group-averaged (n = 6) BOLD responses (mean %signal change) to 96% contrast condition in *experiment 2* (averaged across all 6 luminance levels) plotted as a function of retinotopic eccentricity within early visual cortex. *B*: group-averaged 96% contrast condition luxotonicity (linear regression slope estimate) in *experiment 2* plotted as a function of retinotopic eccentricity within early visual cortex. Abscissa represents the minimum value of each bin, with data binned on a linear scale. Dashed lines denote the boundaries of the voxel selection region of interest. Data are means ± SE across participants.

although areas V2 and V3 also displayed signatures of luminance modulation. Last, a voxelwise analysis of luxotonicity revealed that the recruitment of luxotonic neural populations within a particular visual area was strongest for high stimulus contrast, an effect that diminished within extrastriate cortices. It is important to note that our use of an artificial pupil rules out the possibility that these reported effects were the byproduct of changes in pupil diameter, which would induce spherical aberrations of the ocular lens. Care was also taken to confirm that voxel selection did not include responses driven by local contrast against the background at the stimulus boundaries.

How do luxotonic responses square with standard models of the human visual system? Cortical representations of Michelson contrast are largely believed to be supported by a variety of center-surround neuronal receptive field organizations, with neural activation largely dictated by the stimulation differences between the excitatory and inhibitory components (Movshon et al. 1978; Ringach 2004). A strict interpretation of this framework would predict that the visuocortical response to changes in the overall luminance within a uniform portion of the visual scene should produce no net change in response. This particular prediction emerges because it is assumed that excitatory and inhibitory receptive field components counterbalance one another or are mutually antagonistic (Hubel and Wiesel 1962), so in the absence of a relative feature to drive the visual system, no change would be evoked with overall luminance, a prediction that clearly fails in the context of our current study. However, the luxotonic properties observed in this study can still be integrated with the standard model by assuming instead that there are small, yet true, inherent imbalances that exist between certain excitatory and inhibitory neuronal receptive field components. Even in the absence of local changes in any relative features, with this small adjustment to the standard model, the inherent imbalance would allow for luxotonic responses. Moreover, this inherent imbalance becomes more prominent as one increases the overall luminance of the visual scene, especially under conditions that better approximate our everyday experience. The pattern of the results reported potentially reflects the existence of such an inherent imbalance between excitatory and inhibitory components in early visual cortex, that transitions from a strongly contrast-dependent state seen in V1 and V2 into a contrast-invariant state in V3. Although in general the presence of luxotonic modulation is present throughout all early visuocortical areas, it is interesting to note that luxotonic modulation becomes stronger specifically for low-contrast stimuli in V2 and V3, over which the degree of luxotonic modulation for high- and low-contrast stimuli seemingly converges. The ubiquity of this imbalance throughout the initial tiers of the visual hierarchy, and the subtleties of how it changes between them, should be taken into account as the fundamental response properties and organization of the mammalian visual system are further brought to light.

There is some evidence supporting the idea that inherent imbalances in excitatory and inhibitory receptive field components reside within the visual system at the cortical level (Kremkow et al. 2016; Xing et al. 2010). Some electrophysiology experiments have observed no difference in the contribution of excitatory and inhibitory processes in shaping cat

visuocortical receptive field (RF) properties across multiple luminance levels (albeit at a fixed stimulus Michelson contrast) (Bisti et al. 1977). However, exploratory studies have reported that striate cells with ON-center RF organizations were most likely to be classified as luxotonic (Maguire and Baizer 1982; Ramoa et al. 1985), with the OFF-surround responses becoming weaker relative to ON-center responses under lower luminance conditions (Ramoa et al. 1985). Interestingly, despite these apparent luminance-dependent changes in RF organization, response selectivity to other visual features (i.e., orientation and spatial frequency) remained the same (Ramoa et al. 1985). However, reports of luxotonic striate cells displaying no orientation specificity are also known to exist (Kayama et al. 1979; Maguire and Baizer 1982), and a recent study has shown that spatial frequency selectivity at the cortical level can be modified by stimulus contrast (at low temporal frequencies), with the authors concluding that changes in selectivity can be best explained by an altered balance of excitation and inhibition (Pawar et al. 2019).

Recent evidence from multiunit recordings demonstrated that the ratio between the response strength of excitatory and suppressive components of cortical receptive fields can be differentially modulated by luminance within the lower photopic range (Jansen et al. 2019). A noncortical locus of an excitatory-inhibitory imbalance may originate from a particular type of melanopsin-expressing retinal ganglion cell conferring photosensitive properties operating over a very large range of light intensities (Dacey et al. 2005). The ablation of intrinsically photosensitive retinal ganglion cells (ipRGCs) has been shown to impair contrast sensitivity in mice (Schmidt et al. 2014), and the luminance-mediated melanopsin phototransduction process of certain ipRGCs can alter the intrinsic excitability of the cell (Sonoda et al. 2018). However, the relatively long integration times and sustained responses that characterize these ipRGCs (Dacey et al. 2005; Schmidt et al. 2014) may not be able to reflect the relatively brief onset/offset dynamics of the parametric stimuli presented in the current neuroimaging study. Furthermore, the increased intrinsic excitability with increasing luminance has been shown to preferentially enhance low-contrast responsivity (Sonoda et al. 2018), whereas the current results demonstrate that luminance interacted with contrast responses predominantly at high contrast levels, suggesting that a different process may better account for these effects. Relatedly, we believe it is important to note that the spectral power distribution (SPD) of the projector used to display our stimuli has several discernible peaks (see Sugawara 2004, section 4.4.1), unlike the relatively broad and even SPD typically found under natural lighting conditions. However, the projector SPD peaks (407, 436, 546, and 578 nm) do not coincide with the wavelength sensitivity of melanopsin (480 nm).

When voxelwise luxotonicity in the 96% contrast condition (*experiment 2*) was compared with pRF modeling results, no clear support for any topographic organization was found. It remains to be seen to what degree the RF size bias of luxotonicity that we have reported is contingent on the stimulus-wide spatial frequency of the experimental stimuli. It has been previously reported that the spatial frequency tuning curves of cortical neurons in cat visual cortex maintain a near-constant shape under different scotopic (Bisti et al. 1977) and photopic (Ramoa et al. 1985) luminance conditions, whereas the peak of spatial frequency tuning curves decrease in magnitude and shift toward lower spatial frequencies as luminance is decreased (Bisti et al. 1977; Ramoa et al. 1985). Similar findings have been reported in macaques, where basic tuning properties of V1 neuron receptive fields were stable when studied under photopic and scotopic conditions, with the exception of a general decrease in firing rate from photopic to scotopic viewing conditions (Duffy and Hubel 2007). Therefore, there is reason to believe that selecting a stimulus spatial frequency that matches the mean preferred spatial frequency tuning within a particular region of interest (i.e., human V1) may not necessarily induce stronger luxotonic recruitment and responsivity across a neural population measured with human neuroimaging. However, it is unclear if results from experiments operating largely within, or close to, scotopic luminance domains carry over to broad photopic regimes.

Small-scale recordings demonstrating positive results of luxotonic activity, mostly from scotopic to low photopic luminance ranges, have been previously reported in the lateral geniculate nucleus (LGN) of macaque (De Valois et al. 1962; Marrocco 1972, 1975), cat (Papaioannou and White 1972; Rossi and Paradiso 1999), and squirrel (Gur 1987). The reduced field of view employed for our fMRI data acquisition protocol did not encompass the LGN. Simultaneous fMRI data acquisition of both subcortical and cortical visual areas may provide further insight into the development and emergence of luxotonic responses throughout the human visual system. Additionally, future fMRI luminance studies may greatly benefit from focusing on luminance levels between 50 and 250 cd/m^2, given that luxotonic responses and contrast modulation appear to approach a plateau at higher luminance levels, which could be partially due to intraocular forward light scatter (Patterson et al. 2015; Vos 2003; Westheimer 2006).

The implications of the reported results suggest that luminance level should be considered when experiments are designed and when contrast responses (and potentially other feature-based responses) are compared across experimental conditions and studies. Specifically, our findings indicate that those studying the visual system who are interested in driving potent visually evoked responses may want to consider measuring stimulus responses at higher luminance. There exists the potential to capture more variance existing within the data collected in vision experiments by taking luminance into account during the analysis and interpretation of results. Doing so will serve to improve our understanding of how the human visual system operates, and ultimately how perception is formed within cortex.

ACKNOWLEDGMENTS

We appreciate the helpful feedback and comments provided by Dr. David Somers, as well as members of the Ling laboratory.

GRANTS

This research was funded by National Institutes of Health (NIH) Grant EY028163 (to S. Ling). This research was carried out in part at the Harvard Center for Brain Science. This work involved the use of instrumentation supported by the NIH Shared Instrumentation Grant Program, specifically, NIH Grant S10OD020039.

DISCLOSURES

No conflicts of interest, financial or otherwise, are declared by the authors.

AUTHOR CONTRIBUTIONS

L.N.V. and S.L. conceived and designed research; L.N.V. performed experiments; L.N.V. analyzed data; L.N.V. and S.L. interpreted results of experiments; L.N.V. prepared figures; L.N.V. drafted manuscript; L.N.V. and S.L. edited and revised manuscript; L.N.V. and S.L. approved final version of manuscript.

REFERENCES

Albrecht DG, Geisler WS. Motion selectivity and the contrast-response function of simple cells in the visual cortex. *Vis Neurosci* 7: 531–546, 1991. doi:10.1017/S0952523800010336.

Andersson JLR, Skare S, Ashburner J. How to correct susceptibility distortions in spin-echo echo-planar images: application to diffusion tensor imaging. *Neuroimage* 20: 870–888, 2003. doi:10.1016/S1053-8119(03)00336-7.

Barlow RB Jr, Verrillo RT. Brightness sensation in a ganzfeld. *Vision Res* 16: 1291–1297, 1976. doi:10.1016/0042-6989(76)90056-0.

Bartlett JR, Doty RW Sr. Response of units in striate cortex of squirrel monkeys to visual and electrical stimuli. *J Neurophysiol* 37: 621–641, 1974. doi:10.1152/jn.1974.37.4.621.

Berens P. CircStat: a MATLAB toolbox for circular statistics. *J Stat Softw* 31: 1–21, 2009. doi:10.18637/jss.v031.i10.

Bisti S, Clement R, Maffei L, Mecacci L. Spatial frequency and orientation tuning curves of visual neurones in the cat: effects of mean luminance. *Exp Brain Res* 27: 335–345, 1977. doi:10.1007/BF00235508.

Blakemore C, Campbell FW. On the existence of neurones in the human visual system selectively sensitive to the orientation and size of retinal images. *J Physiol* 203: 237–260, 1969. doi:10.1113/jphysiol.1969.sp008862.

Blakeslee B, McCourt ME. A unified theory of brightness contrast and assimilation incorporating oriented multiscale spatial filtering and contrast normalization. *Vision Res* 44: 2483–2503, 2004. doi:10.1016/j.visres.2004.05.015.

Boyaci H, Fang F, Murray SO, Kersten D. Responses to lightness variations in early human visual cortex. *Curr Biol* 17: 989–993, 2007. doi:10.1016/j.cub.2007.05.005.

Brainard DH. The Psychophysics toolbox. *Spat Vis* 10: 433–436, 1997. doi:10.1163/156856897X00357.

Cohen MA, Grossberg S. Neural dynamics of brightness perception: features, boundaries, diffusion, and resonance. *Percept Psychophys* 36: 428–456, 1984. doi:10.3758/BF03207497.

Cornelissen FW, Wade AR, Vladusich T, Dougherty RF, Wandell BA. No functional magnetic resonance imaging evidence for brightness and color filling-in in early human visual cortex. *J Neurosci* 26: 3634–3641, 2006. doi:10.1523/JNEUROSCI.4382-05.2006.

Cornsweet T. *Visual Perception*. London: Academic, 1970.

Dacey DM, Liao HW, Peterson BB, Robinson FR, Smith VC, Pokorny J, Yau KW, Gamlin PD. Melanopsin-expressing ganglion cells in primate retina signal colour and irradiance and project to the LGN. *Nature* 433: 749–754, 2005. doi:10.1038/nature03387.

Dale AM. Optimal experimental design for event-related fMRI. *Hum Brain Mapp* 8: 109–114, 1999. doi:10.1002/(SICI)1097-0193(1999)8:2/3<109:AID-HBM7>3.0.CO;2-W.

De Valois RL, Jacobs GH, Jones AE. Effects of increments and decrements of light on neural discharge rate. *Science* 136: 986–988, 1962. doi:10.1126/science.136.3520.986.

DeYoe EA, Bartlett JR. Rarity of luxotonic responses in cortical visual areas of the cat. *Exp Brain Res* 39: 125–132, 1980. doi:10.1007/BF00237544.

Duffy KR, Hubel DH. Receptive field properties of neurons in the primary visual cortex under photopic and scotopic lighting conditions. *Vision Res* 47: 2569–2574, 2007. doi:10.1016/j.visres.2007.06.009.

Dumoulin SO, Wandell BA. Population receptive field estimates in human visual cortex. *Neuroimage* 39: 647–660, 2008. doi:10.1016/j.neuroimage.2007.09.034.

Fischl B. FreeSurfer. *Neuroimage* 62: 774–781, 2012. doi:10.1016/j.neuroimage.2012.01.021.

Foley JM, Boynton GM. Forward pattern masking and adaptation: effects of duration, interstimulus interval, contrast, and spatial and temporal frequency. *Vision Res* 33: 959–980, 1993. doi:10.1016/0042-6989(93)90079-C.

Frazor RA, Geisler WS. Local luminance and contrast in natural images. *Vision Res* 46: 1585–1598, 2006. doi:10.1016/j.visres.2005.06.038.

Gardner JL, Sun P, Waggoner RA, Ueno K, Tanaka K, Cheng K. Contrast adaptation and representation in human early visual cortex. *Neuron* 47: 607–620, 2005. doi:10.1016/j.neuron.2005.07.016.

Geisler WS, Albrecht DG, Crane AM. Responses of neurons in primary visual cortex to transient changes in local contrast and luminance. *J Neurosci* 27: 5063–5067, 2007. doi:10.1523/JNEUROSCI.0835-07.2007.

Gilchrist A, Delman S, Jacobsen A. The classification and integration of edges as critical to the perception of reflectance and illumination. *Percept Psychophys* 33: 425–436, 1983. doi:10.3758/BF03202893.

Goodyear BG, Menon RS. Effect of luminance contrast on BOLD fMRI response in human primary visual areas. *J Neurophysiol* 79: 2204–2207, 1998. doi:10.1152/jn.1998.79.4.2204.

Graham N, Sutter A, Venkatesan C. Spatial-frequency- and orientation-selectivity of simple and complex channels in region segregation. *Vision Res* 33: 1893–1911, 1993. doi:10.1016/0042-6989(93)90017-Q.

Greve DN, Fischl B. Accurate and robust brain image alignment using boundary-based registration. *Neuroimage* 48: 63–72, 2009. doi:10.1016/j.neuroimage.2009.06.060.

Gur M. Intensity coding and luxotonic activity in the ground squirrel lateral geniculate nucleus. *Vision Res* 27: 2073–2079, 1987. doi:10.1016/0042-6989(87)90121-0.

Haynes J-D, Lotto RB, Rees G. Responses of human visual cortex to uniform surfaces. *Proc Natl Acad Sci USA* 101: 4286–4291, 2004. doi:10.1073/pnas.0307948101.

Hubel DH, Wiesel TN. Receptive fields, binocular interaction and functional architecture in the cat's visual cortex. *J Physiol* 160: 106–154, 1962. doi:10.1113/jphysiol.1962.sp006837.

Hubel DH, Wiesel TN. Receptive fields and functional architecture of monkey striate cortex. *J Physiol* 195: 215–243, 1968. doi:10.1113/jphysiol.1968.sp008455.

Jansen M, Jin J, Li X, Lashgari R, Kremkow J, Bereshpolova Y, Swadlow HA, Zaidi Q, Alonso JM. Cortical balance between ON and OFF visual responses is modulated by the spatial properties of the visual stimulus. *Cereb Cortex* 29: 336–355, 2019. doi:10.1093/cercor/bhy221.

Kahrilas PJ, Doty RW, Bartlett JR. Failure to find luxotonic responses for single units in visual cortex of the rabbit. *Exp Brain Res* 39: 11–16, 1980. doi:10.1007/BF00237064.

Kay KN, Winawer J, Mezer A, Wandell BA. Compressive spatial summation in human visual cortex. *J Neurophysiol* 110: 481–494, 2013. doi:10.1152/jn.00105.2013.

Kayama Y, Riso RR, Bartlett JR, Doty RW. Luxotonic responses of units in macaque striate cortex. *J Neurophysiol* 42: 1495–1517, 1979. doi:10.1152/jn.1979.42.6.1495.

Kingdom FA. Lightness, brightness and transparency: a quarter century of new ideas, captivating demonstrations and unrelenting controversy. *Vision Res* 51: 652–673, 2011. doi:10.1016/j.visres.2010.09.012.

Kinoshita M, Komatsu H. Neural representation of the luminance and brightness of a uniform surface in the macaque primary visual cortex. *J Neurophysiol* 86: 2559–2570, 2001. doi:10.1152/jn.2001.86.5.2559.

Kremkow J, Jin J, Wang Y, Alonso JM. Principles underlying sensory map topography in primary visual cortex. *Nature* 533: 52–57, 2016. doi:10.1038/nature17936.

Kriegeskorte N, Mur M, Ruff DA, Kiani R, Bodurka J, Esteky H, Tanaka K, Bandettini PA. Matching categorical object representations in inferior temporal cortex of man and monkey. *Neuron* 60: 1126–1141, 2008. doi:10.1016/j.neuron.2008.10.043.

Ling S, Pearson J, Blake R. Dissociation of neural mechanisms underlying orientation processing in humans. *Curr Biol* 19: 1458–1462, 2009. doi:10.1016/j.cub.2009.06.069.

Maguire WM, Baizer JS. Luminance coding of briefly presented stimuli in area 17 of the rhesus monkey. *J Neurophysiol* 47: 128–137, 1982. doi:10.1152/jn.1982.47.1.128.

Mante V, Frazor RA, Bonin V, Geisler WS, Carandini M. Independence of luminance and contrast in natural scenes and in the early visual system. *Nat Neurosci* 8: 1690–1697, 2005. doi:10.1038/nn1556.

Marrocco RT. Maintained activity of monkey optic tract fibers and lateral geniculate nucleus cells. *Vision Res* 12: 1175–1181, 1972. doi:10.1016/0042-6989(72)90105-8.

Marrocco RT. Possible neural basis of brightness magnitude estimations. *Brain Res* 86: 128–133, 1975. doi:10.1016/0006-8993(75)90644-7.

Moeller S, Yacoub E, Olman CA, Auerbach E, Strupp J, Harel N, Uğurbil K. Multiband multislice GE-EPI at 7 tesla, with 16-fold acceleration using partial parallel imaging with application to high spatial and temporal whole-brain fMRI. *Magn Reson Med* 63: 1144–1153, 2010. doi:10.1002/mrm.22361.

Movshon JA, Thompson ID, Tolhurst DJ. Spatial summation in the receptive fields of simple cells in the cat's striate cortex. *J Physiol* 283: 53–77, 1978. doi:10.1113/jphysiol.1978.sp012488.

Papaioannou J, White A. Maintained activity of lateral geniculate nucleus neurons as a function of background luminance. *Exp Neurol* 34: 558–566, 1972. doi:10.1016/0014-4886(72)90050-7.

Patterson EJ, Bargary G, Barbur JL. Understanding disability glare: light scatter and retinal illuminance as predictors of sensitivity to contrast. *J Opt Soc Am A Opt Image Sci Vis* 32: 576–585, 2015. doi:10.1364/JOSAA.32.000576.

Pawar AS, Gepshtein S, Savel'ev S, Albright TD. Mechanisms of spatiotemporal selectivity in cortical area MT. *Neuron* 101: 514–527.e2, 2019. doi:10.1016/j.neuron.2018.12.002.

Peng X, Van Essen DC. Peaked encoding of relative luminance in macaque areas V1 and V2. *J Neurophysiol* 93: 1620–1632, 2005. doi:10.1152/jn.00793.2004.

Press WA, Brewer AA, Dougherty RF, Wade AR, Wandell BA. Visual areas and spatial summation in human visual cortex. *Vision Res* 41: 1321–1332, 2001. doi:10.1016/S0042-6989(01)00074-8.

Ramoa AS, Freeman RD, Macy A. Comparison of response properties of cells in the cat's visual cortex at high and low luminance levels. *J Neurophysiol* 54: 61–72, 1985. doi:10.1152/jn.1985.54.1.61.

Reuter M, Rosas HD, Fischl B. Highly accurate inverse consistent registration: a robust approach. *Neuroimage* 53: 1181–1196, 2010. doi:10.1016/j.neuroimage.2010.07.020.

Ringach DL. Mapping receptive fields in primary visual cortex. *J Physiol* 558: 717–728, 2004. doi:10.1113/jphysiol.2004.065771.

Rossi AF, Paradiso MA. Neural correlates of perceived brightness in the retina, lateral geniculate nucleus, and striate cortex. *J Neurosci* 19: 6145–6156, 1999. doi:10.1523/JNEUROSCI.19-14-06145.1999.

Schmidt TM, Alam NM, Chen S, Kofuji P, Li W, Prusky GT, Hattar S. A role for melanopsin in alpha retinal ganglion cells and contrast detection. *Neuron* 82: 781–788, 2014. doi:10.1016/j.neuron.2014.03.022.

Schweitzer NM. Threshold measurements on the light reflex of the pupil in the dark adapted eye. *Doc Ophthalmol* 10: 1–78, 1956. doi:10.1007/BF00172098.

Smith SM, Jenkinson M, Woolrich MW, Beckmann CF, Behrens TE, Johansen-Berg H, Bannister PR, De Luca M, Drobnjak I, Flitney DE, Niazy RK, Saunders J, Vickers J, Zhang Y, De Stefano N, Brady JM, Matthews PM. Advances in functional and structural MR image analysis and implementation as FSL. *Neuroimage* 23, *Suppl* 1: S208–S219, 2004. doi:10.1016/j.neuroimage.2004.07.051.

Sonoda T, Lee SK, Birnbaumer L, Schmidt TM. Melanopsin phototransduction is repurposed by ipRGC subtypes to shape the function of distinct visual circuits. *Neuron* 99: 754–767.e4, 2018. doi:10.1016/j.neuron.2018.06.032.

Squatrito S, Trotter Y, Poggio GF. Influences of uniform and textured backgrounds on the impulse activity of neurons in area V1 of the alert macaque. *Brain Res* 536: 261–270, 1990. doi:10.1016/0006-8993(90)90034-9.

Sugawara H. *Optical Technology Information Magazine "Light Edge" No. 27 Feature: Discharge Lamp. 4. Basic Knowledge of Each Lamp* [in Japanese]. Tokyo, Japan: Ushio Inc., 2004. https://www.ushio.co.jp/jp/technology/lightedge/200404/100314.html.

Vos JJ. Reflections on glare. *Light Res Technol* 35: 163–175, 2003. doi:10.1191/1477153503li083oa.

Wang WL, Li R, Ding J, Tao L, Li DP, Wang Y. V1 neurons respond to luminance changes faster than contrast changes. *Sci Rep* 5: 17173, 2015. doi:10.1038/srep17173.

Watson AB, Yellott JI. A unified formula for light-adapted pupil size. *J Vis* 12: 12, 2012. doi:10.1167/12.10.12.

Westheimer G. Specifying and controlling the optical image on the human retina. *Prog Retin Eye Res* 25: 19–42, 2006. doi:10.1016/j.preteyeres.2005.05.002.

Wilson HR, McFarlane DK, Phillips GC. Spatial frequency tuning of orientation selective units estimated by oblique masking. *Vision Res* 23: 873–882, 1983. doi:10.1016/0042-6989(83)90055-X.

Xiao F, DiCarlo JM, Catrysse PB, Wandell BA. High dynamic range imaging of natural scenes. *10th Color and Imaging Conference Final Program and Proceedings*. 2002: 337–342, 2002.

Xing D, Yeh CI, Shapley RM. Generation of black-dominant responses in V1 cortex. *J Neurosci* 30: 13504–13512, 2010. doi:10.1523/JNEUROSCI.2473-10.2010.

Xu J, Moeller S, Auerbach EJ, Strupp J, Smith SM, Feinberg DA, Yacoub E, Uğurbil K. Evaluation of slice accelerations using multiband echo planar imaging at 3 T. *Neuroimage* 83: 991–1001, 2013. doi:10.1016/j.neuroimage.2013.07.055.

Yeo BT, Krienen FM, Sepulcre J, Sabuncu MR, Lashkari D, Hollinshead M, Roffman JL, Smoller JW, Zöllei L, Polimeni JR, Fischl B, Liu H, Buckner RL. The organization of the human cerebral cortex estimated by intrinsic functional connectivity. *J Neurophysiol* 106: 1125–1165, 2011. doi:10.1152/jn.00338.2011.

Zurawel G, Ayzenshtat I, Zweig S, Shapley R, Slovin H. A contrast and surface code explains complex responses to black and white stimuli in V1. *J Neurosci* 34: 14388–14402, 2014. doi:10.1523/JNEUROSCI.0848-14.2014.